Muon-Spin Rotation Measurements of the Magnetic Field Dependence of the Vortex-Core Radius and Magnetic Penetration Depth in NbSe$_2$

J. E. Sonier, R. F. Kiefl, J. H. Brewer, J. Chakhalian, S. R. Dunsiger,
W. A. MacFarlane, R. I. Miller, and A. Wong

TRIUMF, Canadian Institute for Advanced Research and Department of Physics and Astronomy, University of British Columbia,
Vancouver, British Columbia, Canada V6T 1Z1

G. M. Luke

Department of Physics, Columbia University, New York, New York 10027

J. W. Brill

Department of Physics and Astronomy, University of Kentucky, Lexington, Kentucky 40506-0055
(Received 19 March 1997)

Muon-spin rotation spectroscopy (μSR) has been used to measure the internal magnetic field distribution in NbSe$_2$ for $H_{c1} \ll H < 0.25H_{c2}$. The deduced profiles of the supercurrent density J_s indicate that the vortex-core radius ρ_0 in the bulk decreases sharply with increasing magnetic field. This effect, which is attributed to increased vortex-vortex interactions, does not agree with the dirty-limit microscopic theory. A simple phenomenological equation in which ρ_0 depends on the intervortex spacing is used to model this behavior. In addition, we find for the first time that the in-plane magnetic penetration depth λ_{ab} increases linearly with H in the vortex state of a conventional superconductor. [S0031-9007(97)03923-9]

PACS numbers: 74.70.Ad, 74.60.−w, 76.75.+i

Although the bulk of superconductivity research in the past decade has been dominated by the study of the high-T_c cuprates, there remain unresolved issues concerning conventional superconductors. In the Meissner state of a conventional *s*-wave superconductor, application of a magnetic field H induces pair breaking, and the ensuing backflow of quasiparticles gives rise to a nonlinear dependence of induced supercurrent with respect to the superfluid velocity [1]. The solution of the corresponding nonlinear London equation gives a penetration depth λ which changes quadratically with H. This has been confirmed experimentally in Sn, In [2] and V$_3$Si [3]. Theoretical predictions in the vortex state are less developed, and the H dependence of λ in the vortex state of a conventional superconductor has never been determined experimentally. Similarly, the H dependence of the vortex-core radius ρ_0 has never been measured in the bulk of a conventional superconductor. In a conventional *s*-wave superconductor, $\rho_0 \sim \xi$ (Ref. [4]), where ξ is the coherence length. Measurements of ρ_0 bear directly on the electronic structure of an isolated vortex and provide a necessary comparison for ongoing studies on high-T_c materials.

NbSe$_2$ is particularly well suited for a μSR study of the vortex state since the geometry of the vortex lattice is well established—thus removing one of the largest experimental uncertainties. Scanning tunneling microscopy (STM) measurements at the surface [5–7] and small angle neutron scattering (SANS) measurements in the bulk [8] have produced high quality images of a nearly perfect triangular lattice with long range order. Also the coherence length and the magnetic penetration depth in NbSe$_2$ are nearly ideal for a μSR investigation of the vortex cores. In particular, the large coherence length and correspondingly small value of H_{c2} (<4 T) imply a large signal from the vortex-core regions at moderate magnetic fields.

Most theoretical calculations have modeled the core structure using Ginzburg-Landau (GL) theory, which is strictly valid only near the superconducting phase boundary. Recently, the field dependence of the vortex-core radius has been determined deep in the superconducting state from the microscopic theory in the dirty limit, by Golubov and Hartmann [9]. The vortex-core radius was found to decrease monotonically with increasing applied magnetic field due to the increased strength of the vortex-vortex interactions. Although the authors reported good agreement with STM measurements [5] at the surface of NbSe$_2$ at $T = 0.6T_c$, ρ_0 was somewhat arbitrarily defined and the uncertainty in the measurements was large. The results were relatively surprising since NbSe$_2$ is a clean superconductor—the ratio of the coherence length to the mean free path in the $\hat{a}$-$\hat{b}$ plane is $\xi_0/l \sim 0.15$ [10]. In the present study, we make a comparison between the vortex-core radius measured by μSR in the bulk of NbSe$_2$ and that determined from the spatial dependence of the supercurrent density J_s in the dirty-limit microscopic theory. The results show that the dirty-limit approximation is invalid, even at $T = 0.6T_c$. The H dependence of ρ_0 is fit to a simple phenomenological equation arising from our observation that both λ_{ab} and the GL parameter κ vary linearly with magnetic field. We also report for the first time, μSR measurements of the H dependence of λ_{ab} in the vortex state of a conventional superconductor. Contrary to the

H^2 dependence in the Meissner state, λ_{ab} shows a strong linear H dependence in NbSe$_2$ over a significant range of applied field.

In a μSR experiment the implanted muon samples the distribution of local magnetic fields in the bulk of a type-II superconductor in the vortex state. One monitors the ensemble averaged muon-spin precession signal. The frequency of precession for any given muon is directly proportional to the local magnetic field at the muon site. Further details regarding the μSR technique may be found elsewhere (see, for example, Ref. [11]). The present μSR study of NbSe$_2$ was performed on the M20 beam line at TRIUMF. The single crystal of NbSe$_2$ used in this experiment had a mass of 43 mg and a surface area of $\sim$30 mm^2. The superconducting transition T_c and $H_{c2}(T = 0)$ determined from magnetization were 7.0 K and 3.5 T, respectively. For details regarding the sample growth, see Ref. [12]. The sample was mounted with its $\hat{c}$ axis parallel to the applied field and beam direction. μSR spectra were recorded under conditions of field cooling in a ^{4}He gas flow cryostat. A cup-shaped veto counter was used to suppress the unwanted background signal from muons which missed the sample [13].

In Fig. 1 the Fourier transforms of the muon precession signal in NbSe$_2$ are shown for different fields at $T = 0.33T_c$. The real amplitude of the Fourier transforms is a good representation of the internal magnetic field distribution from the vortex lattice convoluted with small nuclear dipolar fields. Note the small peak near zero in the
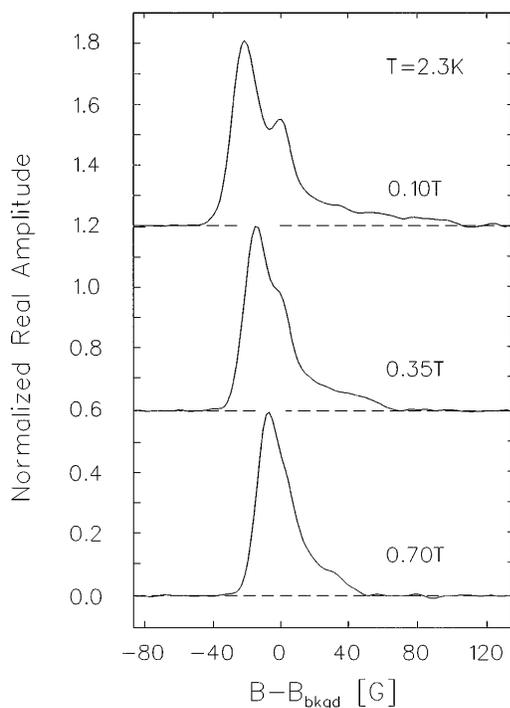
top panel of Fig. 1. This is due to a small (2%) residual background signal due to muons which miss the sample. Line shapes have been renormalized to the same maximum amplitude. The sharp features expected for a perfect triangular vortex lattice, such as the Van Hove singularity at the saddle point, are obscured partly by the broadening effects of the finite Fourier transform and by flux-line lattice disorder. Nevertheless there is a clear high-field cutoff observed in the μSR line shape originating from the finite size of the vortex cores. The effect of increasing H on the high-field cutoff is clearly seen in Fig. 1. At all of the magnetic fields the signal-to-noise ratio of the high-field tail is so large that one can unambiguously extract the vortex-core radius.

In order to test the strength of the pinning forces on the vortex lattice the sample was cooled in an applied field of 0.5 T to 2.3 K, after which the field was decreased by 7.5 mT. In our previous studies of YBa$_2$Cu$_3$O$_{7-\delta}$ [14] we found, under similar conditions, that the background signal shifted to a lower frequency in response to the change in the applied field, while the signal corresponding to muons stopping in the sample remained unchanged. In NbSe$_2$ both signals shifted, indicating that the vortex lattice is considerably more weakly pinned than in YBa$_2$Cu$_3$O$_{7-\delta}$.

The μSR spectra were fitted in the time domain, where there are no complications associated with fitting finite Fourier transforms [15]. The distribution of muon precession frequencies from the vortex lattice was modeled with a theoretical field distribution generated from a GL model [16]. The local field at any point in the $\hat{a}$-$\hat{b}$ plane is given in a suitable approximation by [17]

$$B(\boldsymbol{\rho}) = B_0(1 - b^4) \sum_{\mathbf{G}} \frac{e^{-i\mathbf{G}\cdot\boldsymbol{\rho}}uK_1(u)}{\lambda_{ab}^2 G^2}, \qquad (1a)$$

with

$$u^2 = 2\xi_{ab}^2 G^2(1 + b^4)\left[1 - 2b(1 - b)^2\right]. \qquad (1b)$$

Here B_0 is the average magnetic field, $\mathbf{G}$ are the reciprocal lattice vectors, $b = B_0/B_{c_2}$, ξ_{ab} is the GL coherence length, and $K_1(u)$ is a modified Bessel function. The cutoff factor $uK_1(u)$ accounts for the finite size of the vortex core, whereas, in the London model, $B(\rho)$ diverges logarithmically as $\rho \to 0$. Recently, Yaouanc et al. [17] showed that $uK_1(u)$ is a good approximation of the cutoff factor determined from the exact numerical solutions of the GL equations [18] at low reduced fields b.

The theoretical muon polarization function was generated by assuming the field profile of Eq. (1) and then multiplying by a Gaussian relaxation function $e^{-\sigma^2 t^2/2}$ to take into account any residual disorder in the flux-line lattice and the contribution of the nuclear dipolar moments to the internal field distribution. The residual background signal was fitted assuming a Gaussian broadened distribution of fields. All fitted parameters were treated as independent variables. From the fitted values of σ, the rms deviation of the vortices from their ideal positions in the triangular

FIG. 1. The Fourier transforms of the muon spin precession signal in NbSe$_2$ after field cooling to $T = 0.33T_c$ in magnetic fields of $H = 0.1$, 0.35, and 0.7 T. The average magnetic field of the residual background signal is denoted as B_{bkgd}.

lattice was determined to be less than 3% of the intervortex spacing over the entire field range studied. This small disorder is consistent with STM and SANS imaging experiments on NbSe$_2$.

The magnetic field dependence of λ_{ab} is shown in Fig. 2(a). Contrary to the Meissner state, a linear-H dependence is observed in the field range studied. A fit to the linear relation $\lambda_{ab}(H) = \lambda_{ab}(0)[1 + \beta h]$, where $h = H/H_{c2}(T)$, gives $\lambda_{ab}(0) = 1323$ Å and $\beta = 1.61$ at $T = 0.33T_c$ and $\lambda_{ab}(0) = 1436$ Å and $\beta = 1.56$ at $T = 0.6T_c$. We note that $d[\Delta\lambda/\lambda(0)]/d(H/H_{c2})$ is considerably weaker than for YBa$_2$Cu$_3$O$_{6.95}$ (Ref. [15]), in which there is strong evidence for line nodes in the superconducting energy gap function.

We define an effective vortex-core radius ρ_0 to be the distance from the vortex center for which the supercurrent density $J_s(\rho)$ reaches its maximum value. $J_s(\rho)$ was obtained from fits of the data to Eq. (1) and the Maxwell relation $\mathbf{J}(\boldsymbol{\rho}) = \nabla \times \mathbf{B}(\boldsymbol{\rho})$. In Fig. 3, μSR measurements of ρ_0 are shown as a function of H at $T = 0.33$ (open circles) and $0.6T_c$ (solid circles), along with the STM measurements (open squares) of Ref. [5]. The smaller error bars and reduced scatter in the μSR data reflect the statistical improvement of a μSR experiment which samples a large number of vortices in the bulk of the crystal, as opposed to STM which averages the radius of a few vortices at the surface. The dashed line drawn through the STM results

comes from tunneling current $I(\rho)$ profiles calculated from the Usadel equations, as explained in Ref. [9]. To generate $J_s(\rho)$ profiles from Usadel's dirty-limit theory we extend the work of Ref. [9] to include the self-consistency equation for the vector potential $\mathbf{A}(\rho)$. In cylindrical coordinates the equation of motion is [19]

$$\frac{1}{\rho}\frac{d}{d\rho}\left(\rho\,\frac{d\theta}{d\rho}\right) = \bar{\kappa}^{-2}A^2\sin\theta\cos\theta - \Delta\cos\theta + \omega\sin\theta\,,$$
(2)

where θ parametrizes Usadel's normal ($G = \cos\theta$) and anomalous ($F = \sin\theta$) Green's functions [20], $\Delta(\rho)$ is the order parameter, $\omega = (T/T_c)(2l + 1)$ is the Matsubara frequency and $\bar{\kappa} = [4\pi^5/7\zeta(3)]^{1/2}\kappa$ (where $\kappa = \lambda/\xi$). Equation (2) is supplemented by the following self-consistency equations:

$$\Delta\ln(T/T_c) = -2(T/T_c)\sum_\omega[\Delta/\omega - \sin\theta]\,,$$
(3)

$$J_s(\rho) = \frac{d}{d\rho}\frac{1}{\rho}\left(\frac{d}{d\rho}\rho A\right) = 16\pi\bar{\kappa}^{-2}(T/T_c)A\sum_\omega\sin^2\theta\,,$$
(4)

and the boundary conditions for singly quantized vortices with a Wigner-Seitz cell radius $\rho_s = (\Phi_0/\pi H)^{1/2}$,

$$\Delta(0) = \theta(\omega, 0) = 0\,, \qquad \Delta'(\rho_s) = \theta'(\omega, \rho_s) = 0\,,$$
(5)

$$A(\rho \to 0) \to -\bar{\kappa}/\rho\,, \qquad A(\rho_s) = 0\,.$$
(6)

Equation (2), subject to these boundary conditions, was solved numerically for $\theta(\omega, \rho)$ starting with the initial trial potentials $\Delta(\rho) = \Delta_0\tanh(\rho)$ and $A(\rho) = \bar{\kappa}(1/\rho -$

FIG. 2. The magnetic field dependence of (a) $\lambda_{ab}(H)$ and (b) $\kappa'(H) = \lambda_{ab}(H)/\rho_0(H)$ in the vortex state of NbSe$_2$ at $T = 0.33T_c$ (open circles) and $T = 0.6T_c$ (solid circles). The solid line fits are described in the text.
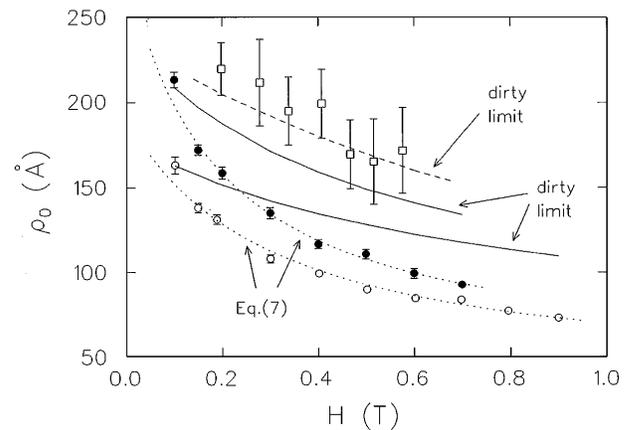
FIG. 3. The magnetic field dependence of the vortex-core radius in NbSe$_2$ determined by STM [5] at $T = 0.6T_c$ (open squares) and by μSR at $T = 0.33T_c$ (open circles) and $0.6T_c$ (solid circles). The solid lines are from calculations of supercurrent density $J_s(\rho)$ profiles using $H_{c2}(0) = 3.5$ T, $H_{c2}(0.33T_c) = 2.9$ T, and $H_{c2}(0.6T_c) = 1.9$ T from magnetization. The dotted lines through the μSR data are from Eq. (7).

ρ/ρ_s^2). Improved values of $\Delta(\rho)$ and $A(\rho)$ were obtained by including the self-consistent conditions (3) and (4). The parameter κ in Eqs. (2) and (4) was determined from fits to the data. We found κ to be nearly temperature independent at all fields studied, which is consistent with the original definition of κ near T_c in GL theory [21]. The deduced values of ρ_0 were not very sensitive to κ. In Fig. 2(b) we define $\kappa' = \lambda_{ab}/\rho_0$, where $\kappa'(H) = 1.06\kappa(H) - 1.98$ and $\kappa'(H) = 1.12\kappa(H) - 1.26$ at $T = 0.33T_c$ and $T = 0.6T_c$, respectively. At both temperatures, κ' (and hence κ) increases linearly with H. Fitting to the linear relation $\kappa'(H) = \kappa'(0)[1 + \gamma h]$, we obtain $\kappa'(0) = 6.9$ and $\gamma = 9.5$ at $T = 0.33T_c$ and $\kappa'(0) = 5.1$ and $\gamma = 10.2$ at $T = 0.6T_c$.

Figure 4 shows the theoretical $J_s(\rho)$ and $\Delta(\rho)$ profiles together with the $J_s(\rho)$ profile obtained from experiment for a particular T and H. The vortex-core radius taken from the $J_s(\rho)$ profiles of the dirty-limit theory are shown as solid lines in Fig. 3. Not surprisingly, there is poor agreement with the μSR data at $T = 0.33T_c$, where thermal smearing of the bound states in the vortex core is negligible. Contrary to the STM results [5], however, there is also poor agreement at $T = 0.6T_c$—suggesting that the dirty-limit theory does not adequately describe the shrinking of the vortex-core radius with increasing H. In the STM experiment it was necessary to arbitrarily define ρ_0 as the radius in which the tunneling current decreased to 36% of $I_{max} - I_{min}$ and $\Delta(\rho)/\Delta(\rho_s) = 1/\sqrt{2}$. However, we find that the $J_s(\rho)$ profiles generated from the dirty-limit theory do not peak exactly at a radius corresponding to $\Delta(\rho)/\Delta(\rho_s) = 1/\sqrt{2}$ for all values of T/T_c and H/H_{c2}. Thus our definition of ρ_0 should provide a better description of the true H dependence of the vortex-core radius. The STM data may also be influenced somewhat by the discontinuity in the energy spectrum of the vortex cores which occurs at the sample surface. It has been suggested that the effect may be an enlargement of ρ_0 [22].

On the other hand, the μSR results fit well (see dotted lines in Fig. 3) to the phenomenological equation,

$$\rho_0(H) = \frac{\lambda_{ab}(H)}{\kappa'(H)} = \rho_0(0)\frac{[1 + \beta h]}{[1 + \gamma h]}, \qquad (7)$$

where $\rho_0(0) = \lambda_{ab}(0)/\kappa'(0)$. From the fits to $\lambda_{ab}(H)$ and $\kappa'(H)$, $\rho_0(0) = 191$ and 282 Å at $T = 0.33$ and $0.6T_c$, respectively. For a triangular vortex lattice $H \cong B_0 = 3\Phi_0/\sqrt{2}L^2$, where L is the intervortex spacing. Thus, for a given temperature, Eq. (7) may be rewritten as a function of the distance between vortices.

In conclusion, we have determined that the magnetic penetration depth λ_{ab} shows a linear magnetic field dependence in the vortex state of NbSe$_2$. The linear term is considerably weaker than that determined previously for YBa$_2$Cu$_3$O$_{6.95}$. Also, we find that the vortex-core radius ρ_0 which shrinks with increasing field is not adequately described by the dirty-limit microscopic theory, but does obey a simple phenomenological equation involving the intervortex spacing. Our results imply that the conventional GL equations, with field-independent length scales, are not applicable deep in the superconducting state.

[1] S. K. Yip and J. A. Sauls, Phys. Rev. Lett. **69**, 2264 (1992).
[2] A. B. Pippard, Proc. R. Soc. London A **203**, 210 (1950); Yu. V. Sharvin and F. Gantmakher, Sov. Phys. JETP **12**, 866 (1961); S. Sridhar and J. E. Mercereau, Phys. Rev. B **34**, 203 (1986).
[3] T. Hanaguri *et al.,* Physica C **246**, 223 (1995).
[4] M. Tinkham, *Introduction to Superconductivity* (McGraw-Hill, New York, 1996), pp. 167–168.
[5] U. Hartmann *et al.,* SPIE Conf. Proc. **1855**, 140 (1993).
[6] H. F. Hess *et al.,* Phys. Rev. Lett. **62**, 214 (1989).
[7] H. F. Hess *et al.,* Phys. Rev. Lett. **69**, 2138 (1992).
[8] P. L. Gammel *et al.,* Phys. Rev. Lett. **72**, 278 (1994).
[9] A. A. Golubov and U. Hartmann, Phys. Rev. Lett. **72**, 3602 (1994).
[10] K. Takita and K. Masuda, J. Low Temp. Phys. **58**, 127 (1985); D. E. Prober *et al.,* Phys. Rev. B **21**, 2717 (1980).
[11] T. M. Riseman *et al.,* Phys. Rev. B **52**, 10 569 (1995).
[12] H. Drulis *et al.,* Phys. Rev. B **44**, 4731 (1991).
[13] J. W. Schneider *et al.,* Phys. Rev. Lett. **71**, 557 (1993).
[14] J. E. Sonier *et al.,* Phys. Rev. Lett. **72**, 744 (1994).
[15] J. E. Sonier *et al.,* Phys. Rev. B **55**, 11 789 (1997).
[16] Z. Hao *et al.,* Phys. Rev. B **43**, 2844 (1991).
[17] A. Yaouanc *et al.,* Phys. Rev. B **55**, 11 107 (1997).
[18] E. H. Brandt, Phys. Rev. Lett. **78**, 2208 (1997).
[19] L. Kramer *et al.,* J. Low Temp. Phys. **14**, 29 (1974).
[20] K. D. Usadel, Phys. Rev. Lett. **25**, 507 (1970).
[21] V. L. Ginzburg and L. D. Landau, Zh. Eksp. Teor. Fiz. **20**, 1064 (1950).
[22] U. Klein, Phys. Rev. B **41**, 4819 (1990).

FIG. 4. The current density and order parameter for $T = 0.6T_c$ and $H/H_{c2}(0.6T_c) = 0.053$. The solid lines are from the dirty-limit microscopic theory while the dashed line is the supercurrent density from a μSR measurement of the field distribution in NbSe$_2$.